

Ultrasound Evaluation of Negative Energy Balance-Induced Fatty Liver in Sheep ^[1]

Wei YANG ¹ Chuang XU ¹ Cheng XIA ¹ Yuanyuan CHEN ¹
Jiasan ZHENG ¹ Xinwei LI ² Guowen LIU ² Xiaobing LI ²

^[1] This work was supported provided by Chinese National Natural Science Foundation (31502133), Natural Science Foundation of Heilongjiang Province of China (C2015043), National Key Technology R&D Program (Grant No. 2012BAD12B03), and National Program on Key Research Project of China (2016YFD0501206)

¹ College of Animal Science and Veterinary Medicine, Heilongjiang Bayi Agricultural University, Daqing, 163319, CHINA

² College of Animal Science and Veterinary Medicine, Jilin University, 5333 Xi'an Road, Changchun 130062, CHINA

Article Code: KVFD-2017-17932 Received: 20.04.2017 Accepted: 07.08.2017 Published Online: 11.08.2017

Citation of This Article

Yang W, Xu C, Xia C, Chen Y, Zheng J, Li X, Liu G, Li X: Ultrasound evaluation of negative energy balance-induced fatty liver in sheep. *Kafkas Univ Vet Fak Derg*, 23 (6): 887-893, 2017. DOI: 10.9775/kvfd.2017.17932

Abstract

Fatty liver disease is a common liver disease in humans and animals alike, and macrofauna are considered an ideal model of fatty liver disease for ultrasonography (US)-based diagnostic research. Here, a model of fatty liver disease in lactating thin-tail sheep induced by negative energy balance was developed by restricted feeding. Ultrasonographic images were divided into the following fat classes according to liver triglyceride concentrations (ratio of triglyceride weight to wet liver weight): healthy liver, <2%; mild hepatic steatosis (HS), ≥2% to 5%; moderate HS, ≥5% to 10%; and severe HS, ≥10%. Characteristics of Ultrasonographic images according to HS severity were evaluated. As the results, mild to severe HS was detected by restricted feeding. The sensitivity of 5 MHz for diagnostic differentiation of healthy liver, and mild, moderate, and severe HS were 66.7%, 60.0%, 66.7%, and 82.5%, respectively, with a moderate κ statistic ranging from 0.667 to 0.735 among observers. The sensitivity of 3.5 MHz for diagnosis of healthy liver, and mild, moderate, and severe HS were 69.7%, 60.5%, 81.5%, and 75.4%, respectively, with moderate κ statistics ranging from 0.575 to 0.684 among observers. The sensitivities of 3.5 and 5 MHz for moderate to severe HS reached 97.4% and 98.2%, respectively. In summary, visualization at 3.5 and 5 MHz was ideal for diagnosis of HS except mild cases with established US diagnostic standards. Furthermore, with the established model, newer methods, such as image digitizing analysis, can be used for US-based diagnosis of fatty liver in further investigations.

Keywords: *Ultrasound, Fatty liver, Sheep, Negative energy balance*

Negatif Enerji Dengesiyle Oluşturulmuş Koyun Yağlı Karaciğerinin Ultrasonografik Değerlendirmesi

Özet

Yağlı karaciğer hastalığı insanlarda ve benzer olarak hayvanlarda yaygın bir karaciğer hastalığı olup, makrofauna yağlı karaciğer hastalığının ultrasonografi (US)-temelli diagnostik araştırmaları için ideal bir modeldir. Bu çalışmada, laktasyondaki ince kuyruklu koyun ırkında negatif enerji dengesi ile yağlı karaciğer hastalığı modeli beslemenin kısıtlaması yoluyla oluşturulmuştur. Ultrasonografik görüntüler karaciğer trigliserid konsantrasyonu (yaş karaciğer ağırlığının trigliserid ağırlığına oranı) baz alınarak yağ sınıflarına ayrılmıştır; sağlıklı karaciğer, <2%; hafif hepatik steatozis (HS), ≥2% ile 5% arası; orta derecede HS, ≥5% ile 10% arası ve şiddetli HS, ≥10%. HS şiddetine göre ultrasonografik görüntülerin özellikleri değerlendirildi. Sonuç olarak kısıtlı besleme ile hafif ve orta derecelerde HS tespit edildi. Sağlıklı, hafif, orta ve şiddetli HS'nin diagnostik ayırımı için 5 MHz'nin hassasiyeti sırasıyla %66.7, %60.0, %66.7 ve %82.5 olarak belirlendi. Gözlemciler arasında ortalama κ istatistik 0.667 ile 0.735 arasında değişim gösterdi. Sağlıklı, hafif, orta ve şiddetli HS'nin diagnostik ayırımı için 3.5 MHz'nin hassasiyeti sırasıyla %69.7, %60.5, %81.5 ve %75.4 olarak belirlendi. Gözlemciler arasında ortalama κ istatistik 0.575 ile 0.684 arasında değişim gösterdi. Orta ve şiddetli HS için 3.5 ve 5 MHz'lerin hassasiyetlikleri sırasıyla %97.4 ve %98.2'ye ulaştı. Özet olarak, 3.5 ve 5 MHz'lerde görüntüleme hafif vakalar haricinde HS'nin tanısı için tespit edilmiş olan US tanı standartlarında idealdir. Ayrıca, bu model görüntü dijital analiz gibi yeni metotlar ile birlikte yağlı karaciğerin US temelli tanısında ileriki araştırmalarda kullanılabilir.

Anahtar sözcükler: *Ultrasonografi, Yağlı karaciğer, Koyun, Negatif enerji dengesi*



İletişim (Correspondence)



+86 431 87836166 (Xiaobing Li), +86 459 6819121 (Chuang Xu)



xbli@jlu.edu.com (Xiaobing Li), Xuchuang7175@163.com (Chuang Xu)

INTRODUCTION

Fatty liver disease is a common in both humans and a variety of mammals, including dairy cows, sheep, dogs, and cats [1,2]. The degree of fatty liver disease ranges from simple hepatic steatosis (HS) to nonalcoholic steatohepatitis (NASH) with or without fibrosis or cirrhosis [3]. Although the correlation between excessive fat intake and non-alcoholic fatty liver disease in humans remains controversial [4], its prevalence has continued to increase concomitant with the epidemic of obesity. In addition, a severe negative energy balance (NEB) during the early lactation period, as a consequence of insufficient energy intake to sustain the high energy requirements for milk production, can also cause fatty liver, especially in dairy cows [5-7], thereby resulting in major economic losses to the dairy industry [8,9].

Although liver biopsy is the gold standard for assessment of fatty liver disease, the procedure is invasive and only evaluates approximately 0.002% of the liver parenchyma [10]. In contrast, ultrasonography (US) is a non-invasive and convenient testing modality with high sensitivity and specificity that is widely used for the diagnosis of fatty liver. US can reflect both metabolic derangements and histological changes caused by HS. However, intra- and inter-observer agreements of US findings are inconsistent across various studies and the diagnostic accuracy of liver US is higher for severe HS than mild HS and NASH [3]. Thus, further research is needed to establish criteria for highly sensitive diagnostic US of fatty liver. In this study, US findings of NEB-induced fatty liver in sheep were evaluated for establishing a practical US diagnostic standard of estimating the degree of fatty liver.

MATERIAL and METHODS

Ethical Approval

The study protocol was approved by the Ethics Committee on the Use and Care of Animals of Heilongjiang Bayi Agricultural University (Daqing, China)

Fatty Liver Model in Lactating Sheep

A total of 14 pregnant thin-tail ewes with parities of 2-3 were acquired. After lambing, the sheep were fasted for 12 h and allowed to nurse for lamb freedom and then allocated to two experimental groups: a control group (CG, $n = 4$), comprised of sheep that gave birth to a single lamb that remained with the ewe in individual pens and received a normal diet of 2 kg of peanut hay and 300 g of a concentrate composed of 2.1 kg of dry matter/day, 12.8 MJ of net energy for lactation (NEL)/day, and 173.7 g of absorbable protein/day twice per day (09:00 and 16:00 h), and a fatty liver model group (MG, $n = 10$), which included six single birth sheep (SMG) and four double birth sheep (DMG) that received a restricted diet of 200 g/

day of peanut hay and 60 g of concentrate composed of 0.4 kg of dry matter/day, 2.6 MJ of NEL/day, and 34.7 g of absorbable protein/twice per day (09:00 and 16:00 h) to supply the ewes with sufficient energy for lactation. Ewes in both groups were fed with the designated diets for 16 days.

Abdominal US

Abdominal US was performed prior to the morning feeding on postpartum days 4, 7, 10, 13, and 16 by a single expert physician. Images were obtained using the SIUI CTS-7700V US system (Shantou Institute of Ultrasonic Instruments Co., Ltd., Shantou, China) with a 2.5-5-MHz curved transducer operated at 3.5 MHz and a 4-8-MHz linear array transducer operated at 5.0 MHz. The following settings of the equipment were fixed and used throughout the study period: depth range of image, 8.7 cm; dynamic range, 80 dB; time gain compensation, neutral (sliders in the center position); overall gain, 66 dB for 3.5 MHz and 80 dB for 5.0 MHz; and transmit focus, 3 cm.

The sheep were examined in the left lateral decubitus position without sedation. After carefully shaving and degreasing the skin with 70% alcohol, transcutaneous US of the liver region was conducted at the 8th-13th intercostal spaces of the right flank of the animal. For diagnosis and grading of the severity of HS, standardized transverse and longitudinal views of the right hepatic lobe, including the right kidney, diaphragm, and intestines, as well as the portal vasculature [11], were obtained.

Liver Biopsy and Histological Analysis

Liver biopsies were performed after liver US on postpartum days 4, 7, 10, 13. Briefly, the incision site was shaved, disinfected, and injected with 1 mL of 2% xylocaine. After 10 min, liver biopsy specimens (approximately 20 mg each) were collected through a 0.5 cm right-side incision between the 11th and 12th rib from the mid-scapula to the tuber coxae using a biopsy paracentesis needle (Cone TZ14-16; Cone Instruments, LLC, Cleveland, OH, USA). The liver biopsy specimens were immediately stored at -80°C for triglyceride analysis using an enzymatic kit (Applygen Technologies, Inc., Beijing, China).

On the final day of the experimental period (postpartum day 16), after liver US, each sheep was anesthetized by intramuscular injection of ketamine hydrochloride (50 mg/kg BW) and xylazine hydrochloride (50 mg/kg BW), and euthanized by exsanguination. After exsanguination, the liver was removed and cleaned with saline, and part of the liver was frozen in liquid nitrogen for Oil Red O staining and triglyceride analysis. The remaining tissue was fixed in 4% formaldehyde for hematoxylin/eosin (H&E) and picosirius red staining.

Imaging Analysis

In this study, 70 US images were obtained from the 14

sheep on postpartum days 4, 7, 10, 13, and 16. Images were subdivided into the following fat classes according to liver triglyceride concentrations (expressed as the ratio of triglyceride weight to wet liver weight.): healthy liver, <2%; mild HS, $\geq 2\%$ to 5%; moderate HS, $\geq 5\%$ to 10%; and severe HS, $\geq 10\%$ [12]. According to the fat classes, the following four widely accepted items were used for image analysis to establish standards for fatty liver grade of sheep [13,14]: echogenicity of liver parenchyma (bright liver) compared with the echogenicity of the renal cortex (L-K contrast), visualization of intrahepatic vessels (vessels blurring), and visualization of the posterior hepatic lobe, including the diaphragm, postcaval vein, rumen, and intestines. Visualization of these image characteristics were classified as absent, slight, intermediate, and marked. Three radiologists evaluated the images according the developed standards for sensitivity, specificity, and kappa analysis.

Statistics Analysis

All data were analyzed using SPSS statistical software (version 19.0; IBM-SPSS, Inc., Chicago, IL, USA). Liver triglyceride concentrations are presented as means \pm SD and differences were identified by repeated measures analysis of variance. A probability (P) value of <0.05 was considered statistically significant. Interobserver agreement was analyzed using κ statistics, where $\kappa < 0.4$ indicated poor agreement, 0.4-0.6, indicated moderate agreement; >0.6-0.8 indicated good agreement, and >0.8-1 indicated excellent agreement.

RESULTS

Triglyceride Analysis and Pathological Changes in the Liver

In this study, 70 liver biopsy samples were obtained for tri-glyceride analysis. As shown in Fig. 1A, the liver triglyceride concentrations of the treated sheep were significantly increased after post-partum day 4 and severe HS was detected in DMG sheep after postpartum day 7. Based on the estimated triglyceride concentrations, the samples were divided into the following hepatic fat classes: healthy liver (n = 22), mild HS (n = 10), moderate HS (n = 19), and severe HS (n = 19) (Fig. 1B).

On postpartum day 16, the sheep were anesthetized and then euthanized by blood-letting from the carotid arteries, and liver were collected for biopsy and histological analysis. As shown in Fig. 2, liver histopathological analysis showed various degrees of hepatic fatty infiltration in MG sheep. When the liver triglyceride concentration was increased, lipid

droplets tended to accumulate in the portal area. Similarly, Oil red O staining clearly revealed the tendency of hepatic fatty infiltration to spread from the liver portal area to the hepatic lobule and, importantly, there was a relative correlation between triglyceride concentration and fatty infiltration. In this study, picosirius red was employed to assess the degree of liver fibrosis and steatohepatitis, which revealed no significant difference in the degree of fibrosis between the two groups [15].

Abdominal US

US was used to image the liver at the 8th-13th intercostal spaces. As show in Fig. 3, the hepatic caudate lobe process and cranial pole of the kidney were imaged at the 12th-13th intercostal spaces, while the distal caudal vein of the right hepatic lobe and the interface between the liver and diaphragm, rumen, and postcaval vein were imaged at the 11th-12th intercostal spaces. Most of the right hepatic lobe, copious veins, portal vein, and the interface between the liver and rumen, intestine, and omasum were imaged in the 10th-11th intercostal spaces, while the liver appeared very narrow at the 8th-10th intercostal spaces. In this study, US was used to observe the liver at the 10th-13th intercostal spaces.

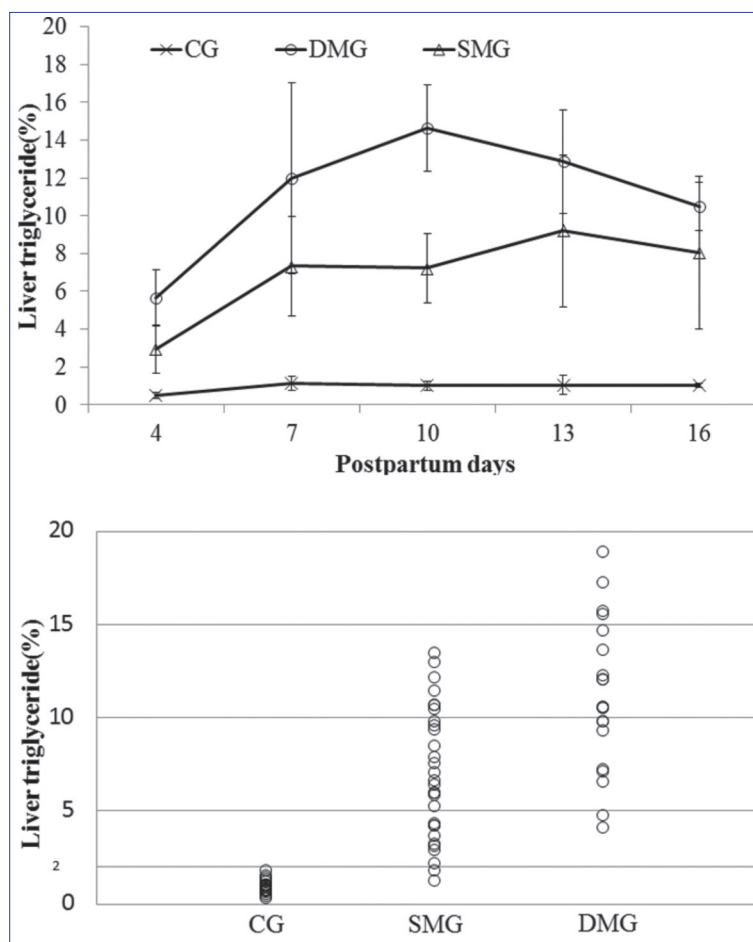


Fig 1. Polygram (A) and scatterplot (B) of sheep liver triglyceride concentration

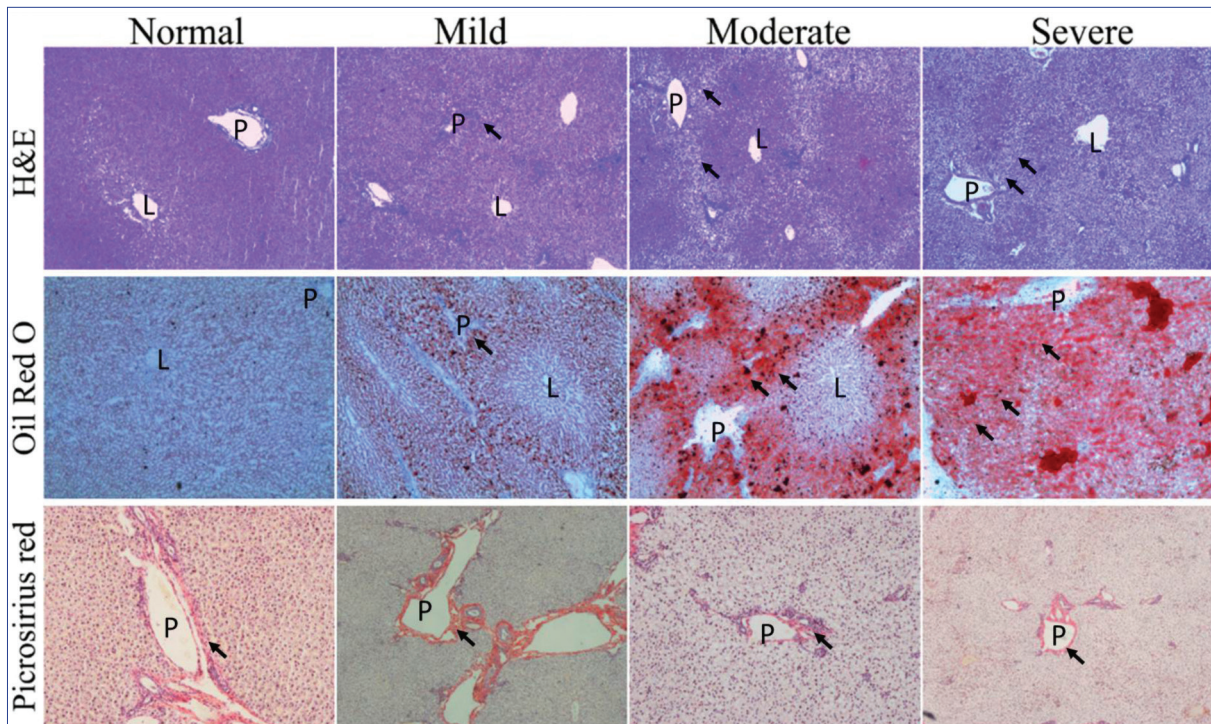


Fig 2. Representative liver pathological images of a healthy liver and those with mild, moderate, and severe HS staining by H & E, oil red O, and picrosirius red. P, hepatic portal area; L, hepatic lobules. H&E and oil red O staining (magnification 40x) show steatosis hepatocytes radially arranged around the portal area (arrows). Picrosirius red staining (magnification 40x) shows only vessels stained in red (arrows)

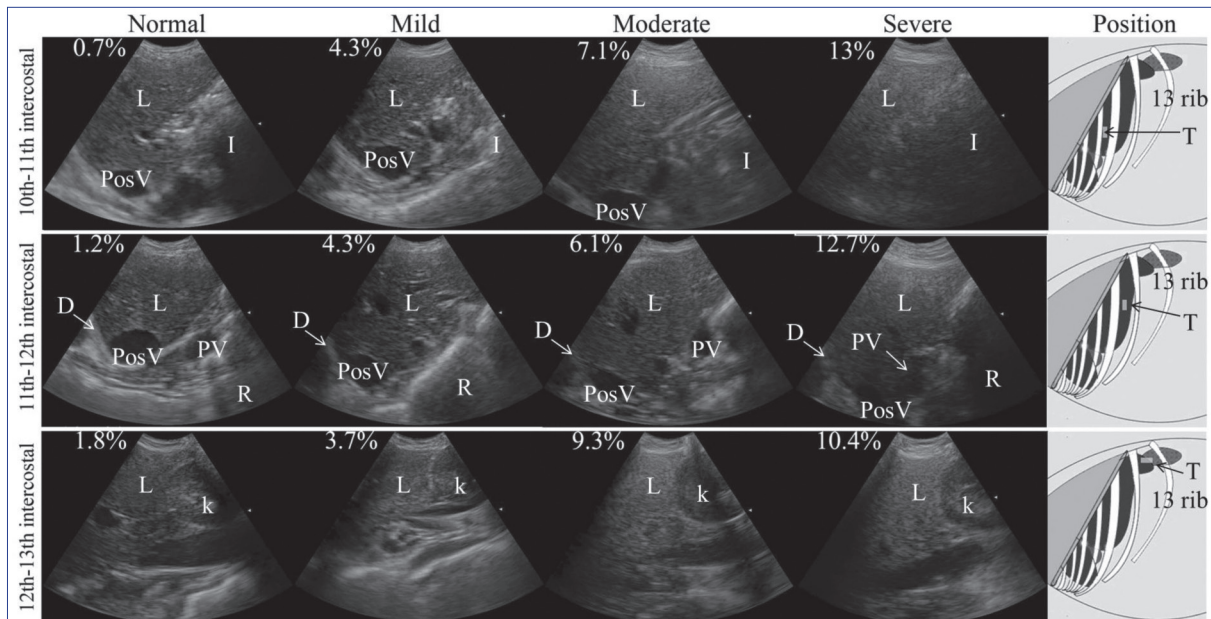


Fig 3. Schematic of image evaluation of fatty liver in sheep, as detected with a 3.5-MHz transducer. The corresponding triglyceride level (%) is shown for each image. L, liver; PosV, postcaval vein; I, intestines; D, diaphragm; PV, portal vein; R, rumen; K, kidney; T, detecting position of the transducer

Imaging Analysis

In this study, an image of a SMG sheep on postpartum day 4, revealed a liver fat concentration of 4.5%, which was eliminated because of unsatisfactory imaging details due to the thickness of the sebum layer, thus 69 images

were included for analysis. In addition, images of L-K contrast could not be obtained with a 5-MHz transducer in this study. As shown in *Fig. 3* and *Fig. 4*, images of a healthy liver showed homogenous hepatic parenchyma, smooth vascular margins, clear hepatic margins, and legible outlines of the organs and tissues around the liver. With mild

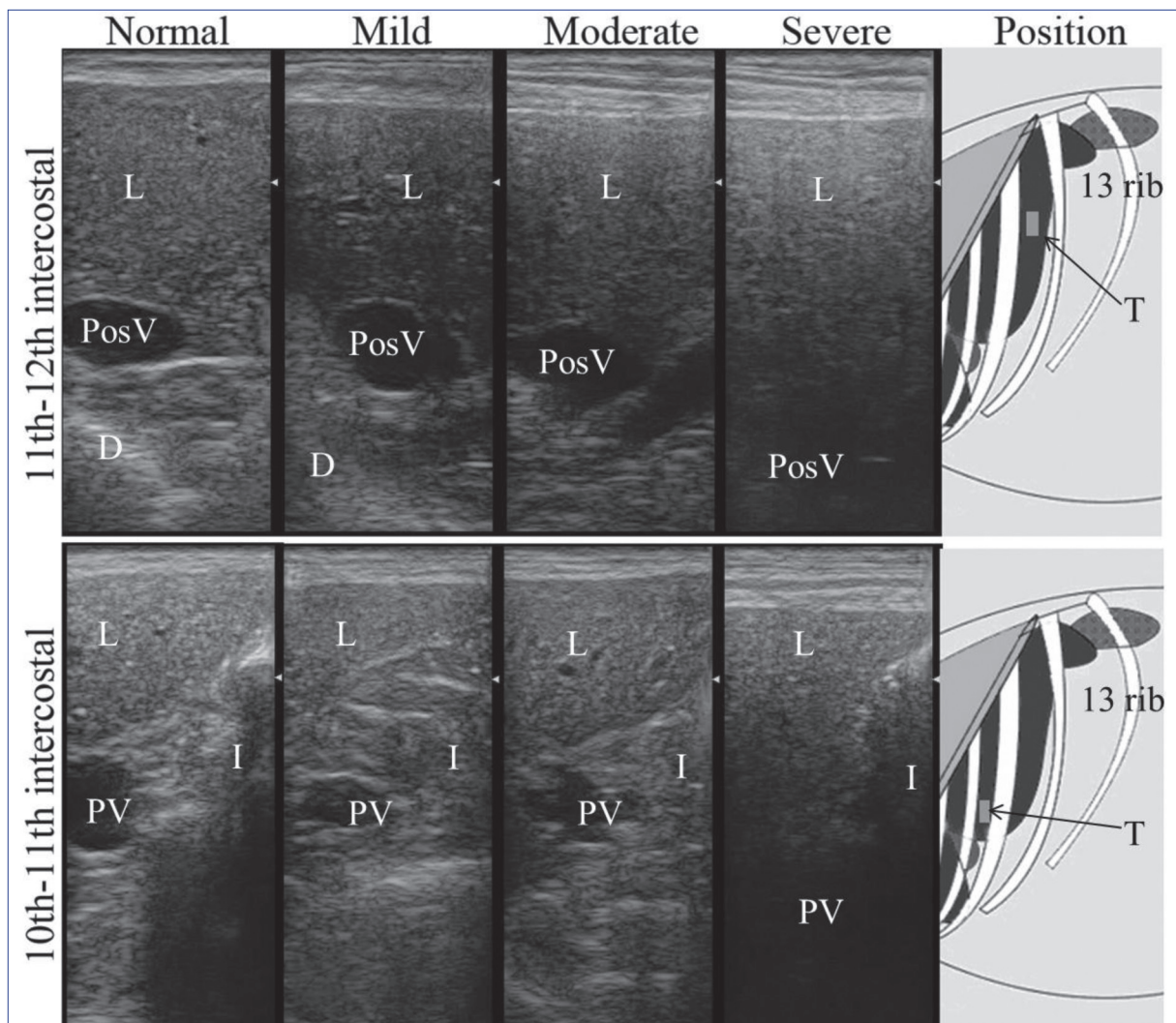


Fig 4. Schematic of image evaluation of fatty liver in sheep, as detected with a 5-MHz transducer. L, liver; PosV, postcaval vein; I, intestines; D, diaphragm; PV, portal vein; T, detecting position of the transducer

Table 1. Sensitivity, specificity, and kappa coefficient values of observers for established US diagnosis standards

Hepatic Steatosis Grade	3.5 MHz		5M Hz	
	Sensitivity (%)	Specificity (%)	Sensitivity (%)	Specificity (%)
Healthy	69.7	94.3	66.7	93.8
Mild	60.5	92.9	60.0	93.4
Moderate	81.5	86.3	66.7	89.3
Severe	75.4	93.3	82.5	84.0
Interobservers agreement (κ)				
Radiologist 1 vs. 2	0.684		0.735	
Radiologist 1 vs. 3	0.575		0.702	
Radiologist 2 vs. 3	0.639		0.667	

HS, US showed a slight increase in L-K contrast and slight attenuation of echogenicity from the distal veins, vena cava, diaphragm, and rumen wall. Imaging of moderate

HS showed intermediate attenuation of the posterior beam, an increase in the echo ratio of the liver and kidney, decreased echo of the mid-field of the liver and intestines, significant attenuation of the echo of the diaphragm in the far end, loss of the vena cava margin, and obvious attenuation of the echo of the rumen. Images of severe HS showed a marked reduction in beam penetration, loss of echoes from most of the portal vein wall, while the ratio of the liver and kidney was marked and unclear to nearly non-visual of the mid-field of the liver and intestine.

Sensitivity, Specificity and Kappa Analysis

A total of 69 US images were evaluated by three observers according to the established diagnostic criteria. As show in *Table 1*, the sensitivity of 5-MHz diagnostic imaging of a healthy liver and those with mild, moderate, and severe HS were 66.7%, 60.0%, 66.7%, and 82.5%, respectively, with moderate κ statistics ranging from 0.667 to 0.735 among observers. The sensitivity of 3.5-MHz diagnostic imaging of a healthy liver and those with mild, moderate, and severe

HS were 69.7%, 60.5%, 81.5%, and 75.4%, respectively, with moderate κ statistics ranging from 0.575 to 0.684 among observers.

DISCUSSION

As a common liver disease in human and animals, fatty liver disease has been widely researched. Several animal models are widely used, such as high-fat diet or gene deletion mice, for studies of the mechanisms of fatty liver disease [16-18]. While macrofauna are considered ideal fatty liver models for US-based diagnosis research, in this study, a model of fatty liver using lactating thin-tail sheep was developed by restricted feeding. After 3 days of restricted feeding, mild to moderate HS was detected. Sheep with multiple births had greater milk yields and developed severe HS after day 7. While there were some limitations for NEB-induced fatty liver, severe NEB caused by insufficient energy intake failed to sustain the high energy demand of colostrum, especially in the early postnatal period. With the long period of restricted feeding management, the milk yield continued to decrease and body fat diminished, while the severity of HS lessened, indicating that hepatic injury caused by long-term HS was limited. In this study, pathological changes to the liver on postpartum day 16 were sufficient to develop a simple HS ovine model.

At present, liver US is widely used for diagnosis of HS in humans. According to widely accepted imaging parameters, US is deemed to be accurate for diagnosis only if the histological extent exceeds 33% [19]. A recent study reported that the pooled sensitivity of US was 84.8% for detection of HS with a histological extent of 20%-30% [20]. In this study, the imaging characteristics of a healthy liver and mild to severe HS were defined, which showed that the diagnostic standard of 3.5 MHz had poor sensitivity for mild HS. As indicated by the results of intra-observer evaluation, due to the severity of HS, part of the image with mild HS was considered to reflect healthy tissue. The image parameters of L-K contrast, far gain attenuation, and vessel blurring for mild HS were unremarkable, while visualization of mild HS at 5 MHz was better than at 3.5 MHz, but still not ideal. The sensitivities of US for moderate and severe HS were lower than previous reports [20], possibly because diseased tissue captured in the image was difficult to distinguish when HS was near 10%. With the established image diagnostic standard in this study, the sensitivity of 3.5 and 5 MHz for moderate to severe HS can reach 97.4% and 98.2%, respectively. Furthermore, with the established model, newer methods, such as image digitizing analysis [21-23], can be used for US-based diagnosis of fatty liver disease.

There were some limitations to US in this study. First, the images were graded according to liver triglyceride content, but some images showing accumulation of liver triglycerides near the train spacing point were usually

difficult to diagnose. The images of severe HS were usually accompanied by a thick sebum layer because obese sheep showed a high degree of fat mobilization in response to restricted feeding that resulted in severe HS, which usually induce attenuation of the echo affecting image evaluation. In addition, different from fatty liver disease caused by a high-fat diet, triglycerides first accumulate around the hepatic lobules, while liver triglycerides of NEB sheep were first detected around the liver portal area [17,24]. Hence, further studies are needed to determine whether the area of triglyceride accumulation impacts the vessel blurring score.

In conclusion, the fatty liver model in lactating sheep induced by restricted feeding was an ideal model for ultrasound and radiology research. Visualization at 3.5 and 5 MHz was an ideal for diagnosis of moderate to severe HS with established US diagnostic standards.

CONFLICT OF INTEREST

The authors declare that they have no competing interests.

REFERENCES

- Gawrieh S, Chalasani N:** NAFLD fibrosis score: Is it ready for wider use in clinical practice and for clinical trials? *Gastroenterology*, 145 (4): 717-719, 2013. DOI: 10.1053/j.gastro.2013.08.025
- Kalaitzakis E, Panousis N, Roubies N, Giadinis N, Kaldrymidou E, Georgiadis M, Karatzias H:** Clinicopathological evaluation of downer dairy cows with fatty liver. *Can Vet J*, 51 (6): 615-622, 2010.
- Ballestri S, Romagnoli D, Nascimbeni F, Francica G, Lonardo A:** Role of ultrasound in the diagnosis and treatment of nonalcoholic fatty liver disease and its complications. *Expert Rev Gastroenterol Hepatol*, 9 (5): 603-627, 2015. DOI: 10.1586/17474124.2015.1007955
- Hu FB, van Dam RM, Liu S:** Diet and risk of Type II diabetes: the role of types of fat and carbohydrate. *Diabetologia*, 44 (7): 805-817, 2001. DOI: 10.1007/s001250100547
- Li Y, Xu C, Xia C, Zhang H, Sun L, Gao Y:** Plasma metabolic profiling of dairy cows affected with clinical ketosis using LC/MS technology. *Vet Q*, 34 (3): 152-158, 2014. DOI: 10.1080/01652176.2014.962116
- Shi X, Li D, Deng Q, Li Y, Sun G, Yuan X, Song Y, Wang Z, Li X, Li X, Liu G:** NEFAs activate the oxidative stress-mediated NF-kappaB signaling pathway to induce inflammatory response in calf hepatocytes. *J Steroid Biochem Mol Biol*, 145, 103-112, 2015. DOI: 10.1016/j.jsbmb.2014.10.014
- Li X, Huang W, Gu J, Du X, Lei L, Yuan X, Sun G, Wang Z, Li X, Liu G:** SREBP-1c overactivates ROS-mediated hepatic NF-kappaB inflammatory pathway in dairy cows with fatty liver. *Cellular Signalling*, 27 (10): 2099-2109, 2015. DOI: 10.1016/j.cellsig.2015.07.011
- Amon E, Allen SR, Petrie RH, Belew JE:** Acute fatty liver of pregnancy associated with preeclampsia: Management of hepatic failure with postpartum liver transplantation. *Am J Perinatol*, 8 (4): 278-279, 1991. DOI: 10.1055/s-2007-999396
- Gill EJ, Contos MJ, Peng TC:** Acute fatty liver of pregnancy and acetaminophen toxicity leading to liver failure and postpartum liver transplantation. A case report. *J Reprod Med*, 47 (7): 584-586, 2002.
- Piscaglia F, Marinelli S, Bota S, Serra C, Venerandi L, Leoni S, Salvatore V:** The role of ultrasound elastographic techniques in chronic liver disease: current status and future perspectives. *Eur J Radiol*, 83 (3): 450-455, 2014. DOI: 10.1016/j.ejrad.2013.06.009
- Bohte AE, Koot BG, van der Baan-Slootweg OH, van Werven JR, Bipat S, Nederveen AJ, Jansen PL, Benninga MA, Stoker J:** US cannot

- be used to predict the presence or severity of hepatic steatosis in severely obese adolescents. *Radiology*, 262 (1): 327-334, 2012. DOI: 10.1148/radiol.11111094
- 12. Bobe G, Young JW, Beitz DC:** Invited review: pathology, etiology, prevention, and treatment of fatty liver in dairy cows. *J Dairy Sci*, 87 (10): 3105-3124, 2004. DOI: 10.3168/jds.S0022-0302(04)73446-3
- 13. Liang RJ, Wang HH, Lee WJ, Liew PL, Lin JT, Wu MS:** Diagnostic value of ultrasonographic examination for nonalcoholic steatohepatitis in morbidly obese patients undergoing laparoscopic bariatric surgery. *Obesity Surgery*, 17 (1): 45-56, 2007. DOI: 10.1007/s11695-007-9005-6
- 14. Saverymuttu SH, Joseph AE, Maxwell JD:** Ultrasound scanning in the detection of hepatic fibrosis and steatosis. *Br Med J*, 292, 13-15, 1986. DOI: 10.1136/bmj.292.6512.13
- 15. Rector RS, Thyfault JP, Uptergrove GM, Morris EM, Naples SP, Borengasser SJ, Mikus CR, Laye MJ, Laughlin MH, Booth FW, Ibdah JA:** Mitochondrial dysfunction precedes insulin resistance and hepatic steatosis and contributes to the natural history of non-alcoholic fatty liver disease in an obese rodent model. *J Hepatol*, 52 (5): 727-736, 2012. DOI: 10.1016/j.jhep.2009.11.030
- 16. Jump DB, Depner CM, Tripathy S, Lytle KA:** Impact of dietary fat on the development of non-alcoholic fatty liver disease in Ldlr-/- mice. *Proc Nutr Soc*, 75 (1): 1-9, 2016. DOI: 10.1017/S002966511500244X
- 17. Suzuki-Kemuriyama N, Matsuzaka T, Kuba M, Ohno H, Han SI, Takeuchi Y, Isaka M, Kobayashi K, Iwasaki H, Yatoh S, Suzuki H, Miyajima K, Nakae D, Yahagi N, Nakagawa Y, Sone H, Yamada N, Shimano H:** Different effects of eicosapentaenoic and docosahexaenoic acids on atherogenic high-fat diet-induced non-alcoholic fatty liver disease in mice. *PLoS One*, 11 (6): e0157580, 2016. DOI: 10.1371/journal.pone.0157580
- 18. Ateş A, Gürsel FE, Altiner A, Bilal T, Erdoğan Ö, Özyoğurtçu H:** Effect of *Garcinia cambogia* extract on fatty liver in rats fed high lipid. *Kafkas Univ Vet Fak Derg*, 17 (6): 1015-1020, 2011. DOI: 10.9775/kvfd.2011.4991
- 19. Saadeh S, Younossi ZM, Remer EM, Gramlich T, Ong JP, Hurley M, Mullen KD, Cooper JN, Sheridan MJ:** The utility of radiological imaging in nonalcoholic fatty liver disease. *Gastroenterology*, 123 (3): 745-750, 2002. DOI: 10.1053/gast.2002.35354
- 20. Hernaez R, Lazo M, Bonekamp S, Kamel I, Brancati FL, Guallar E, Clark JM:** Diagnostic accuracy and reliability of ultrasonography for the detection of fatty liver: A meta-analysis. *Hepatology*, 54 (3): 1082-1090, 2011. DOI: 10.1002/hep.24452
- 21. Ghoshal G, Lavarello RJ, Kemmerer JP, Miller RJ, Oelze ML:** *Ex vivo* study of quantitative ultrasound parameters in fatty rabbit livers. *Ultrasound Med Biol*, 38 (12): 2238-2248, 2012. DOI: 10.1016/j.ultrasmedbio.2012.08.010
- 22. Thijssen JM, Starke A, Weijers G, Haudum A, Herzog K, Wohlsein P, Rehage J, De Korte CL:** Computer-aided B-mode ultrasound diagnosis of hepatic steatosis: A feasibility study. *IEEE Trans Ultrason Ferroelectr Freq Control*, 55 (6): 1343-1354, 2008. DOI: 10.1109/TUFFC.2008.797
- 23. Yoneda M, Suzuki K, Kato S, Fujita K, Nozaki Y, Hosono K, Saito S, Nakajima A:** Nonalcoholic fatty liver disease: US-based acoustic radiation force impulse elastography. *Radiology*, 256 (2): 640-647, 2010. DOI: 10.1148/radiol.10091662
- 24. Bedossa P:** Lesions in nonalcoholic fatty liver disease. *Rev Prat*, 62 (10): 1419, 2012.